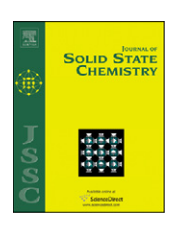
FISEVIER

Contents lists available at SciVerse ScienceDirect

Journal of Solid State Chemistry

journal homepage: www.elsevier.com/locate/jssc



Electronic structure and optical properties of the nonlinear optical crystal $Pb_4O(BO_3)_2$ by first-principles calculations

Zhihua Yang a,*, Shilie Pan a,*, Hongwei Yu a,b, Ming-Hsien Lee c

- ^a Xinjiang Key Laboratory of Electronic Information Materials and Devices, Xinjiang Technical Institute of Physics & Chemistry, Chinese Academy of Sciences, 40-1 South Beijing Road, Urumqi 830011, China
- ^b Graduate School of the Chinese Academy of Sciences, Beijing 100049, China
- ^c Department of Physics, Tamkang University, Taipei 25137, Taiwan

ARTICLE INFO

Article history: Received 16 July 2012 Received in revised form 11 September 2012 Accepted 12 September 2012 Available online 25 September 2012

Keywords: First-principles calculation Nonlinear optical crystal Electronic structure Optical property Lone pair

ABSTRACT

Pb₄O(BO₃)₂ has a layered-type arrangement with optimally aligned BO₃ triangles. The optical band gap is 3.317 eV obtained via the extrapolation method from the UV-vis-IR optical diffuse reflectance spectrum, consequently the absorption edge is about 374 nm. Density functional calculations using a generalized gradient approximation were utilized to investigate the electronic structures and optical properties of Pb₄O(BO₃)₂. The calculated band structures show a direct gap of 2.608 eV, which is in agreement with the experimental optical band gap. A delocalized π bonding of BO₃ triangles and the stereo-effect of the lone pair $6s^2$ of lead cations are studied in electron densities. The birefringence is about 0.039–0.061 with the wavelength larger than about 375 nm. The calculated second-order susceptibility d_{24} =3.5 d_{36} (KDP) which is well consistent with the powder SHG intensity.

© 2012 Elsevier Inc. All rights reserved.

1. Introduction

Borate nonlinear optical (NLO) crystals have attracted considerable attention in laser science and technology due to their high resistance against laser-induced damage and high transparency in the UV region [1-7]. With advantages of boron-oxygen groups, such as $(B_3O_6)^{3-}$ group in β -BaB₂O₄ (BBO), $(B_3O_7)^{5-}$ group in LiB₃O₅ and CsB₃O₅ (LBO, CBO), (BO₃)³⁻ in KBe₂BO₃F₂ (KBBF), provide apparent contributions in refractive indices, birefringence, and second-order susceptibilities [1,2,8,9]. Among these boron-oxygen groups, $(BO_3)^{3-}$ has been confirmed to be an optimally basic structure unit to generate a suitable birefringence and a large second-order susceptibility. Moreover, introducing noncentrosymmetric (NCS) structural units is one way to obtain new structures in the absence of an inverse symmetry and enhance the second harmonic generation (SHG). One typical case is distorted polyhedra with a d^0 cation center (such as V^{5+} , W^{6+} , Nb⁵⁺) [10]. In Na₂TeW₂O₉, for example, a strong distortion of WO₆ octahedra together with TeO₃ produce local polarizations resulting in a large SHG response $(20 \times KDP)$ [11]. The other case is the well-known distortion from the lone pair effect of cations [12]. The lone-pair cations from the third to the seventh main group (such as Sn²⁺, Pb²⁺, Se⁴⁺, Te⁴⁺, I⁵⁺) mostly possess an ns²

E-mail addresses: zhyang@ms.xjb.ac.cn (Z. Yang), slpan@ms.xjb.ac.cn (S. Pan).

or np^2 configurations [12,13]. Therefore, a new phase-matching nonlinear optical material $Pb_4O(BO_3)_2$ (PBO) was synthesized and studied on the structure and crystal chemistry recently [14].

PBO exhibits the combination effects from the π -conjugated property of the (BO₃)³⁻ anionic group and the distortion character of stereochemically active lone pair effect of Pb²⁺ cation. The structure with the planar $(BO_3)^{3-1}$ reminds us of a series of good deep ultraviolet NLO crystals such as KBBF and Sr₂Be₂B₂O₇ (SBBO) [15]. The anionic group of the layered borate material KBBF is $(BO_3)^{3-}$ and $(BeOF)^{5-}$, while $(BO_3)^{3-}$ determines the transparency in the ultraviolet due to its energy gap smaller than (BeOF)5-, and it is phase matchable with the SHG down to 180 nm [16,17]. SBBO has a KBBF structural feature but with a stronger binding between layered structural units, which is considered as a double-layer structure. The SHG response of PBO was measured about three times that of KDP, and PBO has a wide transparent region from the UV to the near IR region with a UV cut-edge 280 nm. Up to now, the relationship between electronic structure and optical properties has not been studied. The effect of the lone pair $6s^2$ in PBO is still unknown. Therefore, the electronic structure, dielectric functions, refractive indices, birefringence and SHG coefficients will be analyzed from firstprinciples calculation in this paper.

The paper is organized as follows: Section 2 is the experimental section, the diffuse reflectance spectroscopy and experimental optical band gap are discussed in this section. In Section 3, the electronic structures will be calculated by the *ab initio*

^{*} Corresponding authors.

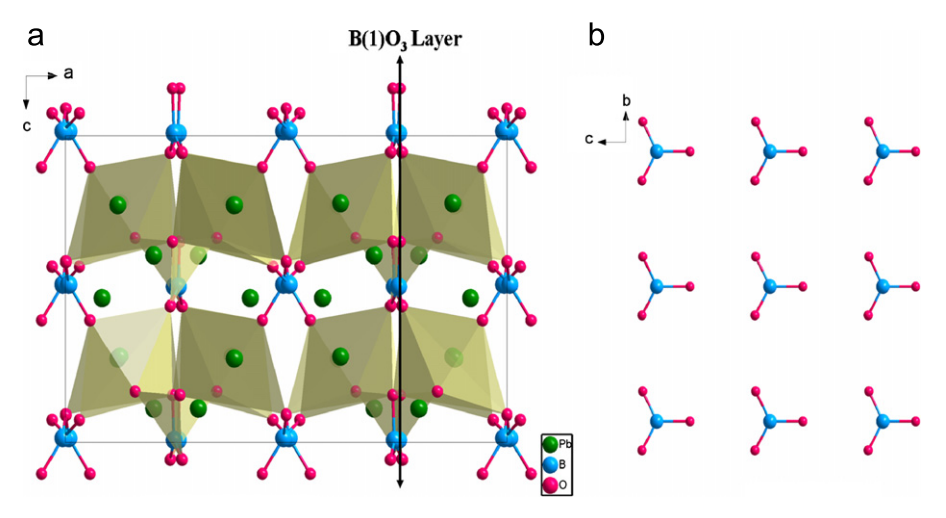


Fig. 1. (a) The 3D network structure of PBO viewed down the b-axis and (b) the arrangement of the B(1)O₃ groups in the (100) direction.

method. In Section 4, the corresponding optical properties will be obtained on the basis of the electronic structures. Summary of results is given in Section 5.

2. Experimental section

PBO has an orthorhombic structure and the space group Aba2 with lattice parameters a=15.4598(16) Å, b=10.8050(11) Å, c=9.9452(11) Å. One can see from Fig. 1(a) that PBO exhibits a complicated three-dimensional (3D) network composed of PbO $_m$ (m=3, 4, 5) polyhedra and BO $_3$ triangles. There are four lead oxygen polyhedra (One PbO $_3$, one PbO $_4$ and two PbO $_5$ polyhedra) interconnecting via corner or edge sharing to form Pb $_4$ O $_{10}$ tetramers. In the 3D network, two kinds of B atoms are observed. B(1)O $_3$ triangles exist in an isolated form, while two B(2)O $_3$ triangles connect each other to form B $_2$ O $_5$ groups. And the isolated B(1)O $_3$ triangles are optimally aligned and adopt a layered-type arrangement (Fig. 1).

The UV–vis–IR optical diffuse reflectance spectrum was measured at room temperature using a Shimadzu Solid Spec-3700DUV spectrophotometer. Data in the energy range 190–2600 nm were collected, reflectance spectrum was converted to absorbance with the Kubelka–Munk function (Fig. 2) [18]. A optical band gap is 3.317 eV obtained via the extrapolation method [19] and consequently the absorption edge is about 374 nm.

3. Electronic structure

To investigate the relationship between microcosmic and macroscopic properties, the electronic structures were obtained using density functional theory (DFT) based *ab initio* calculations implemented in the CASTEP package [20]. The generalized gradient approximation (GGA) with the Perdew–Burke–Ernzerhof functional (PBE) was employed for exchange-correlation potential [21]. A plane–wave basis set energy cutoff was 910 eV within Norm-conserving pseudopotential, and the Monkhorst–Pack [22] scheme was given by $(5 \times 5 \times 7)$ in the irreducible Brillouin zone.

The band structure of PBO calculated along the high symmetry lines is shown in Fig. 3. PBO is a direct gap crystal with a gap from Γ point being 2.608 eV, which is smaller than the experimental optical band gap 3.317 eV due to the discontinuity of the derivative on exchange-correlation energy within density-functional theory [23]. An energy shift in the conduction bands or a so-called scissors operator is introduced for calculating optical responses to overcome

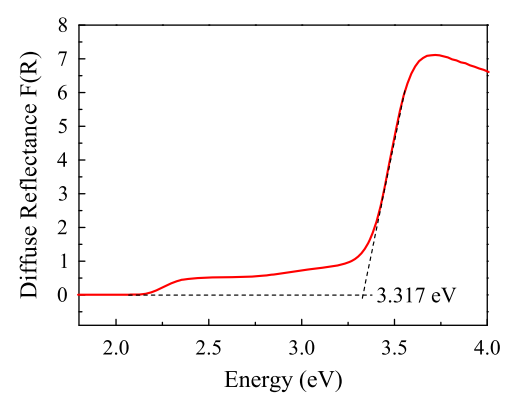


Fig. 2. UV-vis-IR diffuse reflectance spectrum of PBO.

such a difference [24], the corresponding magnitude in our case is 0.709 eV.

The composition and origin of the calculated bands can be understood by analyzing the density of state (DOS) diagrams, shown in Fig. 4. The core states from O, Pb, B contribute the bands below -10 eV, which have been removed from the DOS diagrams for convenience. At the bottom of the valence bands is mainly derived from of the lone pair $6s^2$ of Pb^{2+} and slight from O 2p orbitals. And the top of the valence band is attributed to the hybridization orbitals from B–O groups. The conduction band (CB) is mainly composed of Pb 6s and Pb 6p orbitals, tiny contribution from B 2p and O 2p unoccupied states.

To get more insight into the bonding behaviors of lone pairs of Pb cations and B–O groups, we have plotted the distribution of electron density in the directions shown in Fig. 5. Highly asymmetric lobes on $Pb(1)^{2+}$, $Pb(2)^{2+}$, $Pb(4)^{2+}$ cations reveal stereochemically active lone pair effect of cations. One can see from Fig. 5(b) a typical sp^2 hybridization on B(1) and therefore a delocalization orbital in B(1)O₃ group. The electronic structure indicates that the lead oxygen polyhedra also play an important role in the large SHG effect, except for the contribution from the BO₃ trigonal planes.

4. Optical properties

Due to the low symmetry of PBO (orthorhombic), the dielectric functions in ε^x , ε^y , ε^z are nonzero, Fig. 6 shows real and imaginary parts of dielectric functions ε_1 , ε_2 in the z-direction. The imaginary part ε_2 is calculated in CASTEP numerically by evaluating all the

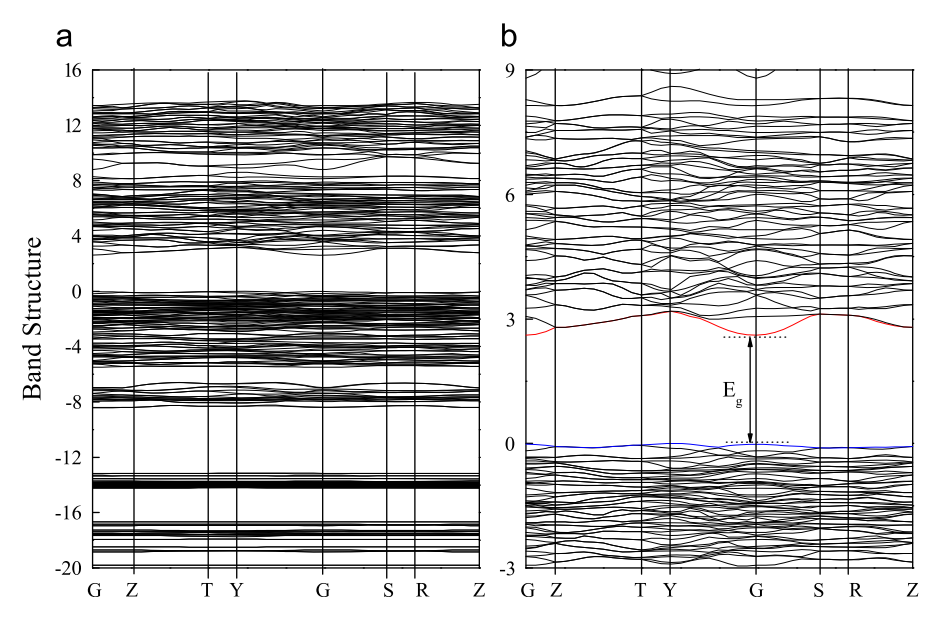


Fig. 3. Calculated band structure of PBO.

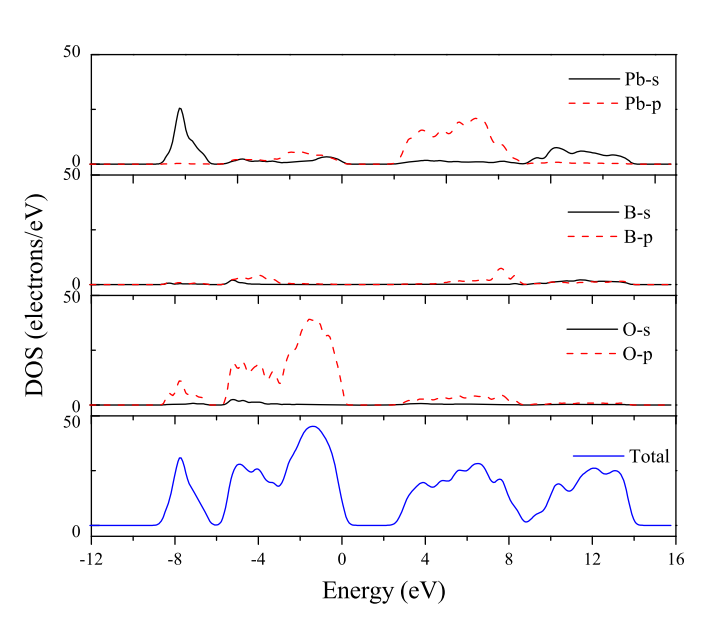


Fig. 4. Total density of states and partial density of states of PBO.

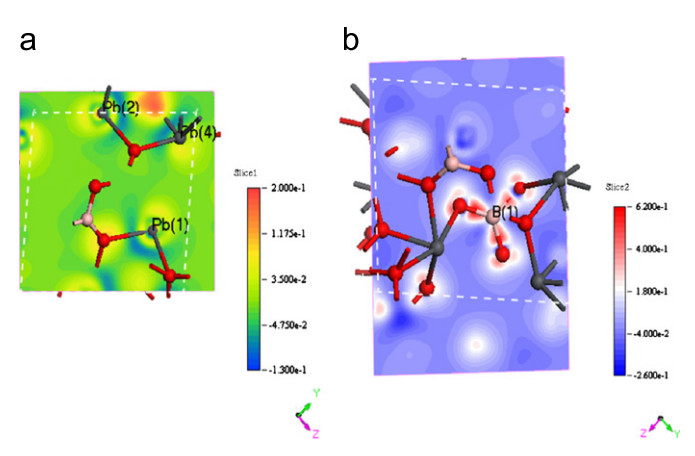


Fig. 5. Electronic densities of $B(1)O_3$ group and Pb^{2+} cations.

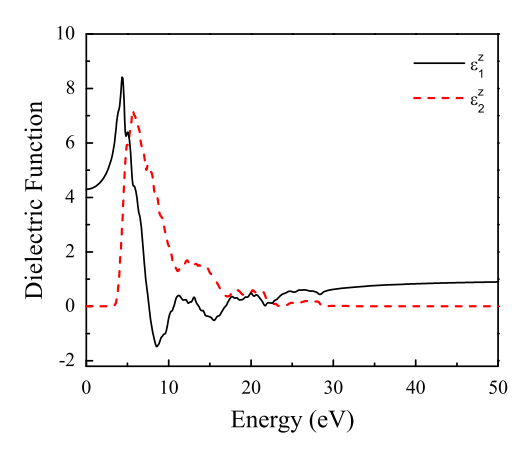


Fig. 6. Dielectric functions for PBO in the *z*-direction.

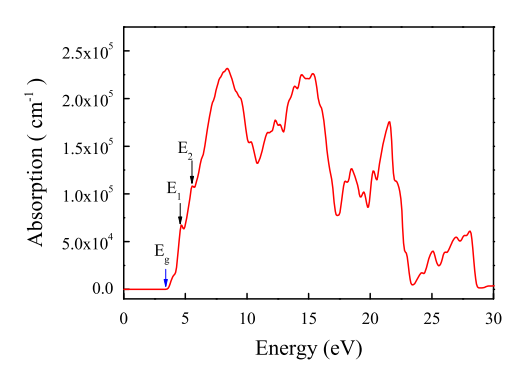


Fig. 7. Absorption spectra of PBO in the z-direction.

transitions from occupied to unoccupied states in the Brillouin zone. The real part ε_1 of the dielectric function is calculated by using the Kramers–Kronig transformation [25]. The imaginary part ε_2 is proportional to the optical absorption of PBO, which indicates absorption when $E > E_g$. Fig. 7 shows that the absorption area region is from ultraviolet area (\sim 374 nm) to high energy absorption area (\sim 40 nm). And E_1 and E_2 represent higher electron transitions.

The calculated refractive indices and the birefringence of PBO are shown in Fig. 8 and Table 1. The corresponding relationship

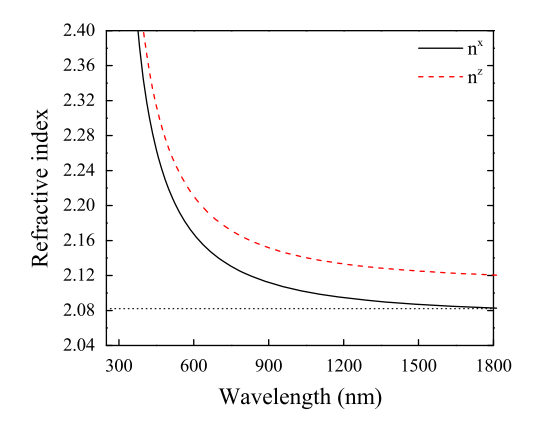


Fig. 8. The maximal and minimal refractive indices depend on the wavelength.

Table 1
The maximal and minimal refractive indices and birefringence of PRO

λ (nm)	n²	n ^x	$\Delta n = n^z - n^x$
375.05490	2.46605	2.40454	0.06151
458.09244	2.30462	2.25516	0.04946
588.35509	2.21532	2.17172	0.04360
715.52014	2.17800	2.13672	0.04128
912.81226	2.15056	2.11094	0.03962
1025.97017	2.14189	2.10279	0.03910

between the crystallographic and the main optical axes are $X \rightarrow n^z$, $Y \rightarrow n^y$, $Z \rightarrow n^x$. One can see the birefringence, which is defined as $n^z - n^x$, is about 0.039–0.061 with the wavelength of about 375 nm.

To investigate the NLO properties of PBO, we calculated the second-order susceptibility d_{ij} coefficients in the static limit in the length gauge [26]. The calculated tensor components d_{15} , d_{24} and d_{33} are 0.16 pm/V, 1.37 pm/V and -0.57 pm/V, respectively. The largest SHG coefficient d_{24} is about 3.5 times that of KDP (d_{36} =0.39 pm/V), which is in good agreement with the experiment powder SHG intensity.

5. Conclusion

The energy structure, density of states, electron densities and optical properties for PBO were studied by density functional theory. It was found that PBO is a direct gap material with the value of 2.608 eV, which is well consistent with the experimental optical band gap. A delocalized bonding of BO₃ triangles and the stereo-effect of the lone pair of Pb²⁺ cation were shown in electron densities. In addition, the birefringence is about 0.039–0.061 with the wavelength of about 375 nm. And the largest NLO coefficient is about 3.5 times that of KDP, which is in good agreement with powder SHG intensity. The calculated electronic

structures and optical properties indicate that the BO $_3$ group with typical delocalization π orbitals and strongly distorted lead oxygen polyhedra with highly asymmetric lobes on lead cations become the origins for the large SHG effect.

Acknowledgments

This work was supported by the "National Natural Science Foundation of China" (Grant Nos. 50802110, 21001114, 11104344), the "One Hundred Talents Project Foundation Program" of Chinese Academy of Sciences, the "Western Light Joint Scholar Foundation" Program of Chinese Academy of Sciences.

References

- [1] C.T. Chen, B.C. Wu, A.D. Jiang, G.M. You, Sci. Sin. Ser. B 28 (1985) 235–243.
- [2] C.T. Chen, Y.C. Wu, A.D. Jiang, G.M. You, R.K. Li, S.J. Lin, J. Opt. Soc. Am. B 6 (1989) 616–621.
- [3] Y.C. Wu, T. Sasaki, S. Nakai, A. Yokotani, H. Tang, C.T. Chen, Appl. Phys. Lett. 62 (1993) 2614–2615.
- [4] Y. Mori, I. Kuroda, S. Nakajima, T. Sasaki, S. Nakai, Appl. Phys. Lett. 67 (13) (1995) 1818.
- [5] J.G. Mao, H.L. Jiang, K. Fang, Inorg. Chem. 47 (2008) 8498–8510;
 J.H. Zhang, F. Kong, J.G. Mao, Inorg. Chem. 50 (2011) 3037–3043.
- [6] F. Kong, S.P. Huang, Z.M. Sun, J.G. Mao, W.D. Cheng, J. Am. Chem. Soc. 128 (2006) 7750–7751.
- [7] P.S. Halasyamani, D. O'Hare, Chem. Mater. 10 (1998) 646–649;
 P.S. Halasyamani, K.R. Poeppelmeier, Chem. Mater. 10 (1998) 2753–2769;
 P.S. Halasyamani, R.J. Francis, S.M. Walker, D. O'Hare, Inorg. Chem. 38 (1999) 271–279;
- E.A. Muller, R.J. Cannon, A.N. Sarjeant, K.M. Ok, P.S. Halasyamani, A.J. Norquist, Cryst. Growth Des. 5 (2005) 1913–1917.
- [8] L. Mei, X. Huang, Y. Wang, Q. Wu, B.C. Wu, C.T. Chen, Z. Kristallogr. 210 (1995) 93–95
- [9] C.T. Chen, G. Liu, Ann. Rev. Mater. Sci. 16 (1986) 203–243;
 N. Ye, Q.X. Chen, B.C. Wu, C.T. Chen, J. Appl. Phys. 84 (1998) 555–556;
 C.T. Chen, Y.C. Wu, R.K. Li, Int. Rev. Phys. Chem. 8 (1989) 65–91.
- [10] K.M. Ok, P.S. Halasyamani, D. Casanova, M. Llunell, S. Alvarez, Chem. Mater. 18 (2006) 3176–3183.
- [11] J. Goodey, J. Broussard, P.S. Halasyamani, Chem. Mater. 14 (2002) 3174–3180.
- [12] P.S. Halasyamani, Chem. Mater. 16 (2004) 3586–3592.
- [13] M. Atnasov, D. Reinen, J. Phys. Chem. A 105 (2011) 5450-5467.
- [14] H. Yu, S. Pan, H. Wu, W. Zhao, F. Zhang, H. Li, Z. Yang, J. Mater. Chem. 22 (2012) 2105–2110.
- [15] C.T. Chen, Y.B. Wang, B.C. Wu, K.C. Wu, W.L. Zeng, L.H. Yu, Nature 373 (1995) 322–324.
- [16] C.T. Chen, Y. Wang, Y. Xia, B.C. Wu, D.Y. Tang, K. Wu, W. Zeng, L.H. Yu, J. Appl. Phys. 77 (1995) 2268–2272.
- [17] B.C. Wu, D.Y. Tang, N. Ye, C.T. Chen, Opt. Mater. 5 (1996) 105-109.
- P. Kubelka, F. Munk, Z. Tech. Phys. 12 (1931) 593–601;
 J. Tauc, Mater. Res. Bull. 5 (1970) 721–731.
- [19] O. Schevciw, W.B. White, Mater. Res. Bull. 18 (1983) 1059-1068.
- [20] S.J. Clark, M.D. Segall, C.J. Pickard, P.J. Hasnip, M.J. Probert, K. Refson, M.C. Payne, Z. Kristallogr. 220 (2005) 567–570.
- [21] J.P. Perdew, K. Burke, M. Ernzerhof, Phys. Rev. Lett. 77 (1996) 3865-3868.
- [22] H.J. Monkhorst, J.D. Pack, Phys. Rev. B 13 (1976) 5188–5192.
- [23] J.P. Perdew, M. Levy, Phys. Rev. Lett. 20 (1983) 1884-1887.
- [24] Z.H. Levine, D.C. Allane, Phys. Rev. B 43 (1991) 4187–4207.
- [25] F. Wooten, Optical Properties of Solid, Academic, New York, 1972.
- [26] J. Lin, M.H. Lee, Z.P. Liu, C.T. Chen, C.J. Pickard, Phys. Rev. B 60 (1990) 13380–13389.